CONTRIBUTIONS REGARDING A FLUID BARRIER SUPER CIRCULATION TECHNIQUE

Valeriu DRAGAN[1], Virgil STANCIU[2]

This paper discusses and tests a new technique for super-circulation without the use of the Coandã effect. The method used is numerical, parametric tests were made on a conventional airfoil with and without the proposed fluid barrier. Results indicate that the principle can be applied on the entire range of conventional angles of attack, providing substantially higher section loadings while maintaining a high lift to drag ratio. Although experimental validation is required, the tests described here may be used as a baseline for this technique. If validated, the fluid barrier may be as an alternative to conventional flaps.

Keywords: Super circulation, Coandã effect, RANS k-epsilon, high lift device

1. Introduction

In calculating lift, L, the Kutta-Jukowsky theorem Ref [1] states that the circulation Γ around the airfoil of the wing has a definitive role, as seen in Eq.1:

$$L=V_{\infty}\Gamma\rho_{\infty} \tag{1}$$

A simple way to understand circulation is the difference between the far field velocity and the velocity near the airfoil as given in Ref [2]. It is therefore intuitive that, for conventional high lift devices, in order to increase lift one must either decrease the velocity of the underside flow or increase the velocity of the top of the wing flow.

Conventional super circulation techniques Ref [3-5] involve blowing a high speed thin jet over the top of the wing – by which the stalling angle is also increased- to increase circulation.

Another, more advanced, method is to use the so-called entrainment principle Ref [6-8] by which a thin jet of air is blown near the trailing edge and entrains a larger current from the top of the wing. Entrainment has been considered a more realistic application than the Upper Surface Blowing (USB) due to its simpler requrements, i.e. the engine can remain in the same

[1]Ph.D.Stud., Depart. Aerospace Sciences, Faculty of Aerospace Engineering, University POLITEHNICA of Bucharest, Romania, e-mail: drvaleriu@gmail.com
[1] Prof. Depart. Aerospace Sciences,Faculty of Aerospace Engineering, University POLITEHNICA of Bucharest, Romania, e-mail: vvirgil.stanciu@yahoo.com

conventional position and the mass flow requirements are generally lower. Figure 1 depicts a generic airfoil designed to operate with the entrainment principle Ref [6], some similar geometries have been tested in Ref [9]. As can be seen, there are two major drawbacks with this desing:

1. The circulation control must be active at all times in order to maintain the boundary layer attachment on the semi-circular ramp.

2. Due to the Coandã effect, the static pressure on the semi-circular ramp is substantially lower than the ambient pressure Ref [10-12].

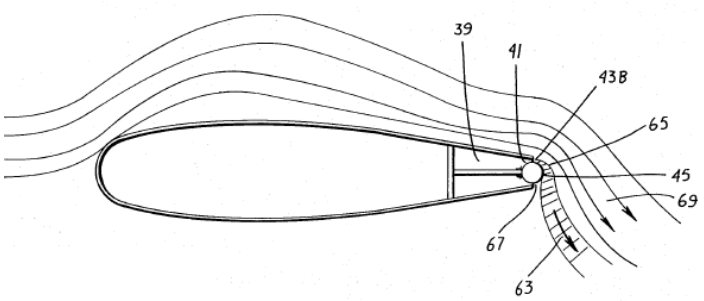

Fig. 1 Airfoil design with entrainment effect; the trailing edge must have circulation control at all times to avoid high drag due to its thickness (US4682746 Thomas, Andrew S.W.)

One solution to this problem is to use an elliptic trailing edge as suggested in Ref [13], however this will adversely influence the super circulation performance of the system.

The current paper tries to introduce a new technique of increasing circulation by use of a so-called fluid barrier on the inner side of the airfoil.

2. The concept of the fluid barrier

Figure 2 illustrates a NACA airfoil using a fluid barrier in order to obtain higher lift by super circulation. It can be seen that the thin jet emerging from the back of injector blocks the ambient airflow, slowing it down. Since the total pressure of the airflow must be constant (with minor lossess due to pressure recovery efficiency), the static pressure in the region near the injector will tend to increase as the dynamic pressure decreases.

The main advantage of using a fluid barrier instead of a solid one is that there is only little additional drag to the airfoil. Figure 3 shows a detail with the static pressure distribution near the injector. The resulting drag of the proposed airfoil at various injector velocities for 0º angle of attack is summarized in table 1 as a fraction of the total drag of the original, un-altered NACA airfoil.

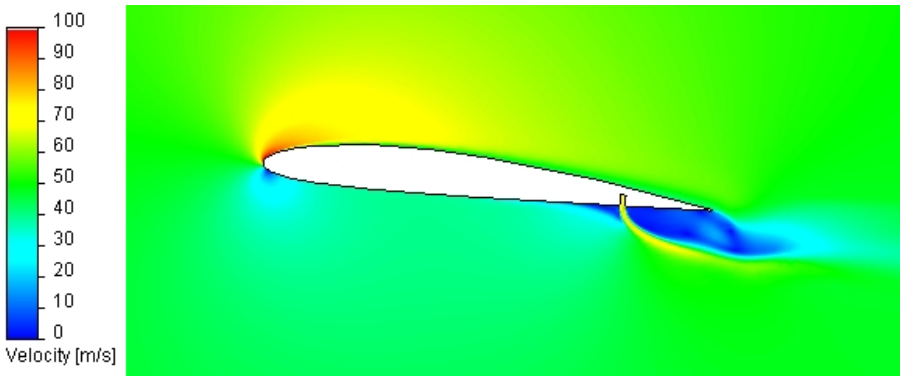

Fig.2 Velocity plots around a NACA 2410 airfoil using the proposed fluid barrier super circulation method 6º angle of attack, $V_{inj} = 1.5V_{\infty}$

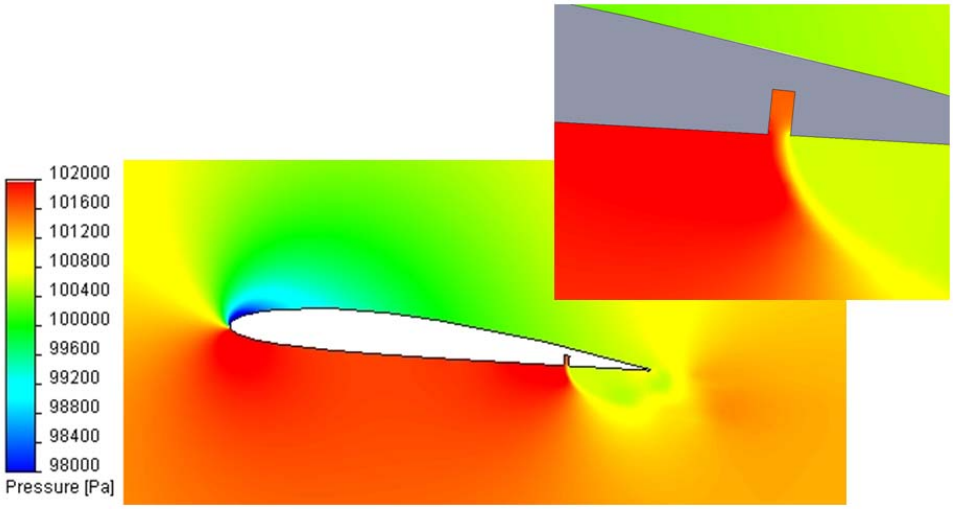

Fig.3 Pressure plot and detail near the fluid barrier injector, 6º angle of attack, $V_{inj} = 1.5V_{\infty}$

Tabel 1

Total drag induced by the proposed system/NACA original drag

Case	Drag %
NACA 2410	100
$V_{inj} = 0.5V_{\infty}$ (25 m/s)	123.351
$V_{inj} = V_{\infty}$ (50 m/s)	162.039
$V_{inj} = 2V_{\infty}$ (100 m/s)	202.222

3. The Computational Fluid Dynamics parametric studies performed

The CFD tests were carried out using the realizable k-epsilon Reynolds Averaged Navier-Stokes model. The choice was made considering that the k-epsilon model is typically more robust in the far field (outside the boundary layer) than the Wilcox k-omega model, Ref [14]. The realizable variation of k-epsilon is generally regarded as the most advanced Ref [15] as it can account for higher wall curvatures and rotational flows which we deal with in this paper. Reynolds's 5 equation stress model was not considered, although it is the most physically-accurate, because it's long convergence time. Reference [16] shows a CFD test of the configuration depicted in Fig.1 using the same k-epsilon realizable turbulence model with satisfactory results. However, the method for circulation control proposed in our paper differs from all entrainment airfoils present in the literature. The key difference being that the blowing is largely perpendicular to the ambient flow instead of tangential to a rounded, blunt trailing edge. This acts as a fluid barrier on the inner surface of the airfoil instead of generating air entrainment on the upper surface. The secondary entrainment effect – discussed further on – which is obtained is of a different nature from the classical one. In our case, the entrainment is due to the formation of a low pressure vortex downstream of the trailing edge which sucks air towards it, whereas in the classical entrainment shown in Fig.1, the air suction is due to the Coandã jet on the rounded trailing edge. As stated, our configuration eliminates the need for a thick rounded trailing edge, making the airfoil more aerodynamic for the cruise flight where there is no fluidic blowing.

A Cartesian mesh was used, as seen in Ref [17] this form of structured mesh offers advantages in meshing small features – such as our injector – and also requires a lower number of cells which decreases computational time. A detail of the mesh used for one of the tested cases is presented in Fig. 4.

The airfoil used is a NACA 2410 with the chord C=1m, the CFD simulations were 2D and the free stream velocity of 50 m/s, ISA atmospheric conditions.

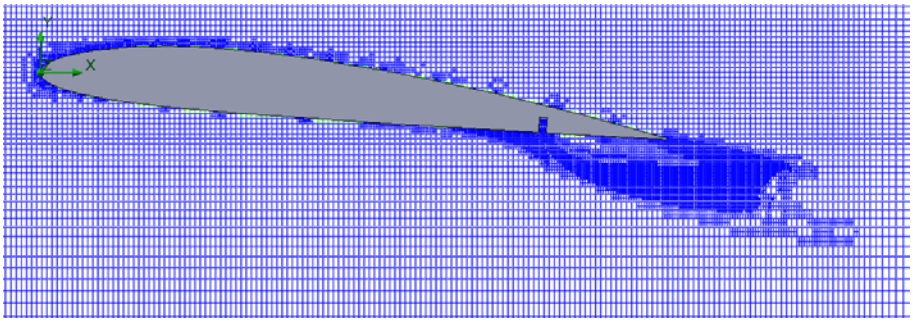

Fig.4 The adapted computational mesh used for a 6º angle of attack with the injector at 80% of the aerodynamic chord

3.2. Optimizing the position of the injector

In order to establish a sound geometric model for the considered airfoil we sat out a series of positional tests in which the injector was placed towards the trailing edge at a progressive distance from the leading edge of the airfoil at 50%C, 60%C, 70%C and 80%C. The 90% distance proved to be too close to the trailing edge and the geometry of the airfoil was too thin to accommodate a real injector.

A first battery of tests was performed at a 0° angle of attack (AoA) with two velocity inlet conditions on the injector: 50 m/s (1/1 of the free stream velocity) and 100 m/s (2/1 of the free stream velocity). The integrated aerodynamic parameters are presented in Table 2.

The total L/D is the Lift to Drag ratio considering the lift provided by the injector, Eq.3 while F_Z and F_X are the Lift and Drag of the airfoil surface. The same notations are used to describe section loading Eq.4.

$$\left(\frac{L}{D}\right)_{Total} = \frac{F_Z + \sin\alpha \cdot [A_{injector} \cdot (P_{static\_injector} - P_{atmbient}) + \dot{m} \cdot v_{injector}]}{F_X + \cos\alpha \cdot [A_{injector} \cdot (P_{static\_injector} - P_{atmbient}) + \dot{m} \cdot v_{injector}]} \quad (3)$$

$$\left(\frac{L}{A_{airfoil\_section}}\right)_{Total} = \frac{F_Z + \sin\alpha \cdot [A_{injector} \cdot (P_{static\_injector} - P_{atmbient}) + \dot{m} \cdot v_{injector}]}{A_{airfoil\_section}} \quad (4)$$

Tabel 2

Fluid barrier parameters variations with injector position

0 AoA 50 m/s	L/D aerodynamic	L/D total (with the jet)	Loading aerodynamic	Loading total (with jet)
80%	78.21620003	82.38433184	796.5037724	833.8784946
70%	52.46259493	55.45751181	758.6229573	796.9409638
60%	34.72038132	37.06770347	643.638168	682.9513478
50%	23.91684932	25.8499444	517.3249954	555.6429332
5 AoA 50 m/s	L/D aerodynamic	L/D total (with the jet)	Loading aerodynamic	Loading total (with jet)
80%	50.00059038	46.3805737	1519.308506	1545.726977
70%	40.14160974	37.81846024	1434.706691	1461.673535
60%	44.50153688	41.0705882	1210.30066	1238.728863
50%	47.4299734	42.45744689	931.7550537	961.8672202

Intuitively, an optimization can be made by maximizing the aerodynamic lift obtained as a result of the fluid barrier, i.e. the influence of the jet lift is minimized. This can be mathematically expressed by Eq.5, which calculates the "Lift to Drag effectiveness":

$$\eta_{L/D}=(F_Z/F_X)/(L/D)_{total} \quad (5)$$

The same principle can be applied to the section loading parameters, a similar expression being Eq.6 named "Section Loading Effectiveness":

$$\eta_{Load}=L/L_{total} \quad (6)$$

A final criterion can be total effectiveness, expressed in Eq.7:

$$\eta_{total}= (\eta_{L/D}\ \eta_{Load})/100 \quad (7)$$

Figs. 5 and 6 show plots of Lift to Drag effectiveness and Load effectiveness for the first battery of tests. The optimal position appears to be the one closest to the trailing edge: 80%.

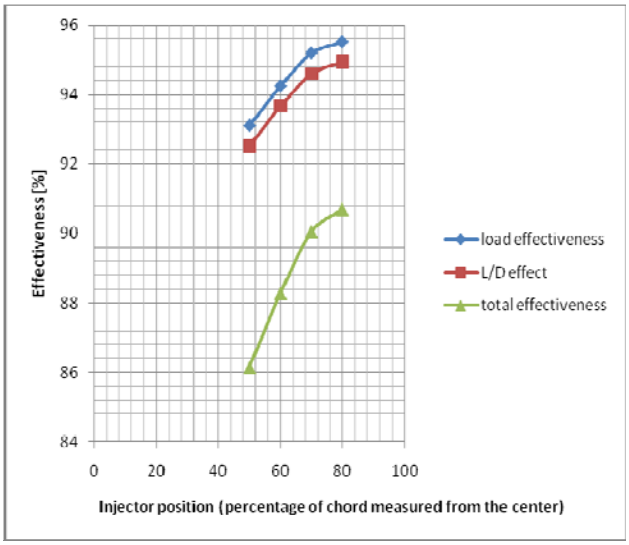

Fig.5 Effectiveness plots for various injector positions at 50 m/sec ($V_{inj}=V_\infty$) injector velocity and 0° Angle of attack.

Observations:

1. The fluid barrier obtains the expected effect of transforming the dynamic pressure of the free stream into static pressure near the airfoil by slowing the incoming air. The most effective position is nearer the trailing edge. The effectiveness curve levels off at around 70-80% of the Chord.

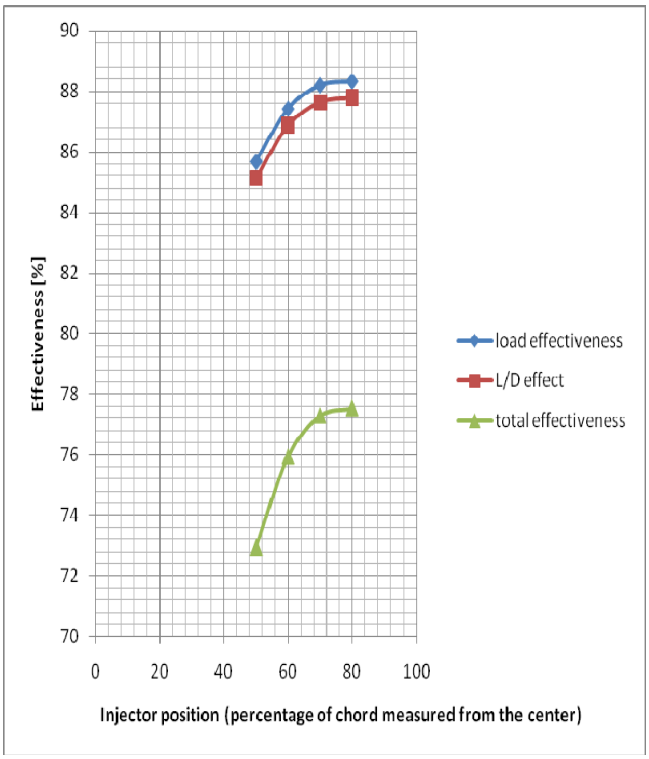

Fig.6 Effectiveness plots for various injector positions at 100 m/sec ($v_{inj}=2v_{\infty}$)injector velocity and 0° Angle of attack.

2. A secondary super circulation effect becomes apparent when the injector is placed near the trailing edge. Air flowing over the top of the airfoil is accelerated towards the trailing edge due to a low pressure region caused by the fluid barrier. This effect is shown in Fig. 7 where we compare a NACA airfoil with and without the fluid barrier.

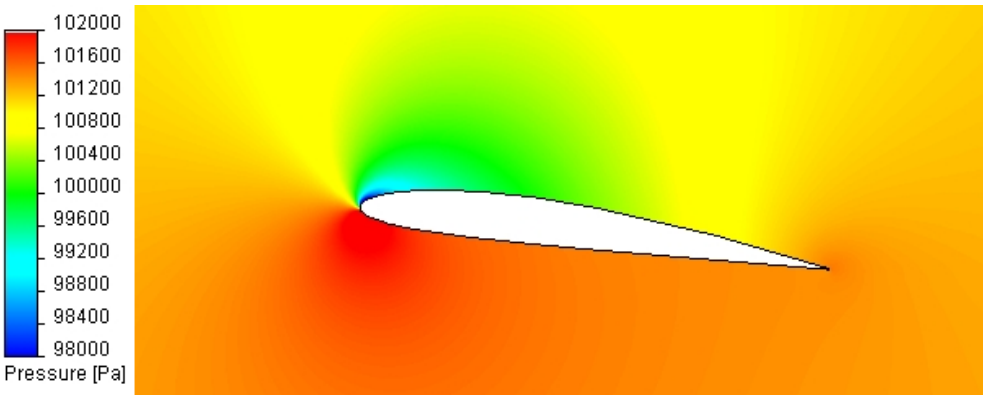

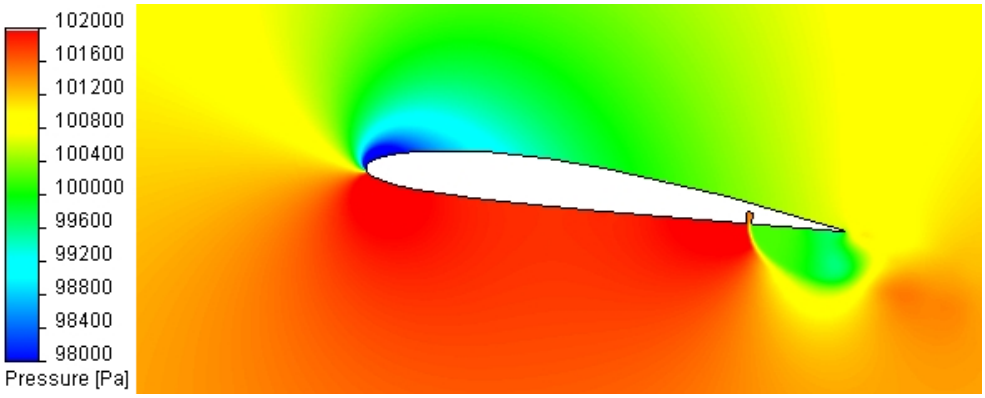

Fig.7 The influence of the fluid barrier on the static pressure near the underside of the airfoil; the secondary super circulation is visible, due to upper side acceleration, the pressure drop on the top of the airfoil is also higher.

3.3. Injector velocity parametric test.

Following the findings in section 2.3. another series of CFD tests were made to establish an optimal velocity at which the air forming the fluid barrier should be injected. This time, both 0° and 6° angles of attack were tested. The results are synthesized in Table 3.

As expected, both lift to drag and section loading increase as the injector velocity is increased. Although for the 0° AoA cases, the lift to drag ratio apears unusually high, this tendency decreases dramatically as the angle of attack increases. This is due to the following factors:

1. The induced drag (lift drag) in the 0° case is basically identical for the NACA airfoil both with and without the fluid barrier while the lift is substantially larger in the fluid barrier case. For higher angles of attack, the overpressure generated by the fluid barrier inherently generates an induced drag component which moderates the $(L/D)_{total}$ ratio. This is shown in Figs. 8 and 9.

2. At higher velocities and low angles of attack, the low pressure region downstream generated by the fluid barrier leads to an accelerated flow over the top of the wing. We shall see that this tendency rapidly decreases as the angle of attack is increased.

Tabel 3

Lift and Drag of the airfoil as a function of injector velocity (aerial velocity is 50 m/s)

Case	loading	loading with jet	lift/drag	lift/drag with jet
normal NACA 2410 0°	267.375804	267.3758043	40.8594034	40.85940339
injector velocity 25 m/s	448.63052	464.0081649	33.708753	35.07450229
injector velocity50 m/s	807.501577	849.9429538	75.7189466	79.69864945
injector velocity100 m/s	1089.82104	1231.886404	134.243529	152.658453

normal NACA 2410 6°	1152.633737	1152.633737	36.04636899	36.04636899
injector velocity 50 m/s	1585.338285	1615.535922	40.30469587	37.33537488
injector velocity75 mps	1884.905897	1957.664462	44.10710187	38.1510256
injector velocity100 mps	1986.304729	2118.036903	54.74601024	41.3986815

The influence of the angle of attack on aerodynamic loading is less visible, as seen in Fig. 10, the fluid barrier outperforms the conventional airfoil at both 0° and 6 AoA, having a linear dependency to the injector velocity.

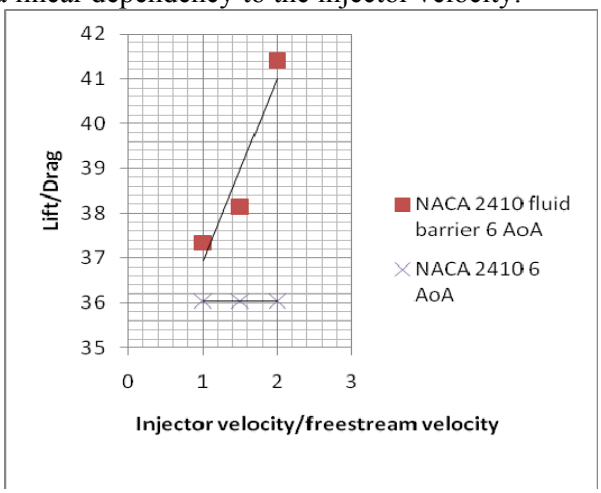

Fig.8 Lift to Drag ratio vs. injector relative velocity (V_{inj}/V_{∞}) 6º angle of attack

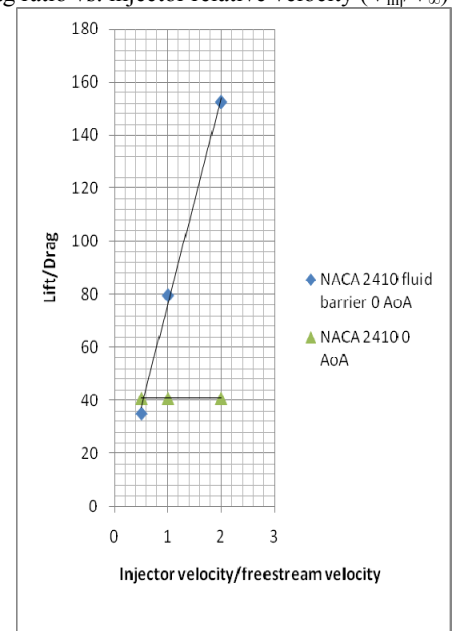

Fig.9 Lift to Drag ratio vs. injector relative velocity (V_{inj}/V_{∞}) 0º angle of attack

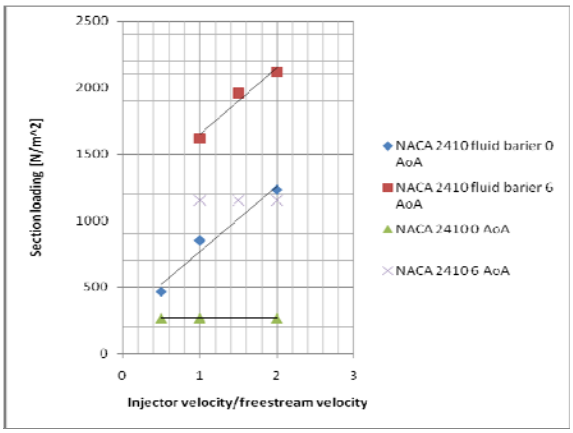

Fig.10 Section Loading vs. injector relative velocity (V_{inj}/V_{∞}) 6º angle of attack

3.4. Lift to drag vs. Angle of attack

Since it has been shown that the fluid barrier method works well at an injector velocity equal to that of the free stream, the next series of tests will be carried out at this speed. The key angles chosen are 0° ,5° , 6° , 7.5° , 10°. The 5° and 7.5° represent the maximum L/D angle and maximum C_L angle as shown in Ref [7], beyond the 7.5° the L/D rapidly deteriorates due to trailing edge stall. Figures11 and 12 depict relative (as a percentage of the maximum value) L/D and Loading charts.

We can observe that the only case where the L/D is substantially higher than normal is the 0° fluid barrier case. Another point in which this ratio is better than the normal NACA airfoil is beyond 7.5° which means that the fluid barrier somehow delays the trailing edge stalling process. As opposed to the L/D ratio, the Loading parameter is significantly higher in all the fluid barrier cases by a margin of ~20%. This means that all cases obtained super circulation by slowing down the airfoil on the underside of the airfoil whereas the 0° case obtain additional lift by a secondary super circulation phenomenon on the top side of the airfoil.

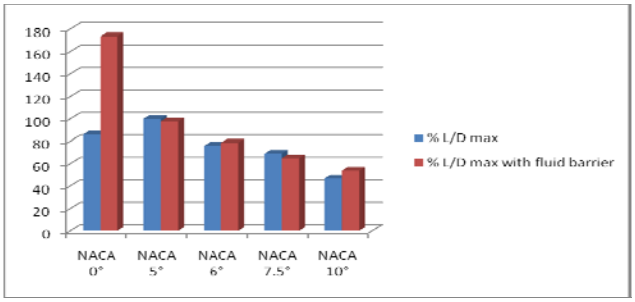

Fig.11 Relative Lift to Drag ratio vs. angle of attack ($V_{inj}=V_{\infty}$)

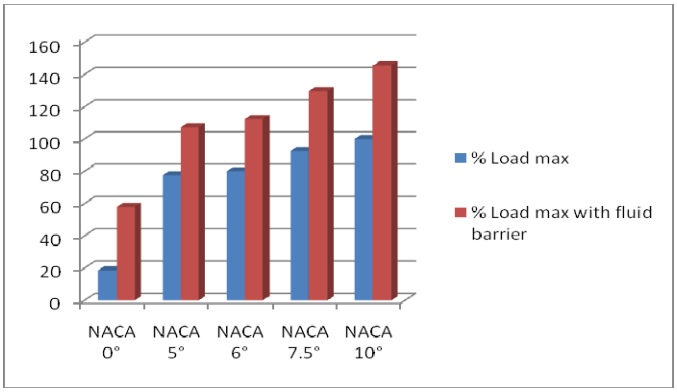

Fig.12 Relative Section Loading vs. angle of attack ($V_{inj}=V_{\infty}$)

4. Conclusions

The current paper introduces a new method for circulation control trough the use of thin fluidic jets perpendicular to the airfoil underside. The concept relies on the capacity of a thin fluid jet to influence the surrounding airflow near an airfoil. The state of the art supercirculation airfoils have the configuration presented in Fig.1. As it can be seen, the trailing edge must have a large radius, making it unpractical for cruise flight due to increased drag. This is one of the major problems preventing the implementation of the technique in real applications. Our design seeks to eliminate this inconvenience by blowing the jet so that it behaves like a fluid barrier on the underside of the airfoil, slowing down the free stream air and creating a high pressure aria which increases lift. Due to the fact that the airfoil shape is the same as the original (initial) airfoil, there is no additional drag associated with the here-by technique.

For testing the proposed configuration we used the same CFD turbulence model used by other authors in testing the state of the art supercirculation airfoil, the realizable k-epsilon model. As indicated, the realizable version of k-epsilon is one of the most advanced RANS models, being able to cope with both flow rotation and flows over curved surfaces.

After establishing a sound means to test our proposed configuration using CFD simulations, the next step was to try and determine some optimal parameters for the geometry and the blowing of the fluidic jet.

In order to find those optimal parameters, the following parametric tests were carried out:

1. Injector position optimization, in which the location of the fluid barrier injector was varied to 50%, 60%, 70% and 90% of the chord, towards the trailing edge (the 80% being the closest to the trailing edge). It was found that:

a. The lift to drag ratio is higher as the injector is placed closer to the trailing edge. The effectiveness, $\eta_{L/D}$ curve, defined by Eq.5 levels off at around 70-80% of the Chord. Hence an optimal position would be at 80% of the Chord.

b. Due to the influence of the fluid barrier, a low pressure bubble is generated near the trailing edge which causes air from the upper side of the airfoil to accelerate. This in itself is a secondary super circulation effect which is more obvious at low angles of attack.

2. Injector velocity, by which it was sought to test the impact of the fluid barrier velocity on the lift to drag ratio and also section loading. Two sets of tests were done, at 0° and 6° angles of attack, for velocities ranging from V_∞ to 2 V_∞. It was concluded that:

a. In the 0° AoA case, the fluid barrier obtained unusually high L/D ratios while in the 6° AoA case, this tendency was greatly reduced.

b. For injector velocities equal to V_∞, the super circulation effect is still useful in the sense that it generates high L/D ratios and significantly higher section loadings.

3. The influence of the angle of attack was the theme of the last test. Here the NACA airfoil was tested with and without the fluid barrier at various angles of attack including the critical 5° (maximum L/D angle) and 7.5° (maximum lift coefficient angle). The injector velocity was equal to the free stream velocity, V_∞.

a. The lift to drag ratio is substantially increased by the fluid barrier only at the 0° angle of attack. The only other angles for which the barrier provides a higher ratio is beyond the 7.5°. This is proof that the fluid barrier delays the natural tendency of trailing edge stalling.

b. Section loading was improved by ~20% for all tested cases, largely regardless of the angle of attack.

Although the results must be treated with caution until experimental validation is obtained, the tests carried out set up a baseline on which one can mount further physical tests. Because of the simplicity of the design, the proposed system does not require special variations of viscosity models such as other super circulation techniques that rely on the Coandã effect Refs.[18-20]. Hence further CFD testing can be made more easily and the results can be more reliable.

R E F E R E N C E S

[1] *Kuethe, A. M. and Chow, C.-Y.*, Foundations of Aerodynamics: Bases of Aerodynamic Design, John Wiley and Sons, Inc., (2006)

[2] *Daniel P. Raymear* Aircraft Design-A Conceptual Approach, second ed. AIAA, (1992)

[3] *B Saeed, G Gratton*, "Exploring the aerodynamic characteristics of a blown annular wing for vertical/short take-off and landing applications", Proceedings of the Institution of Mechanical Engineers, Part G: Journal of Aerospace Engineering June vol. 225 no. 6 689-707 (2011)

[4] *Gregory S. Jones, Robert J. Englar*, Flow Physics and Control Branch NASA Langley Research Center, "Advances In Pneumatic-Controlled High-Lift Systems Through Pulsed Blowing" AIAA 2003-3411 (2003)

[5] *Abramson, J.* "Characteristics of a Cambered Circulation Control Airfoil Having Both Upper and Lower Surface Trailing Edge Slots." Naval Surface Warfare Center – Carderock Division, Bethesda, MD, (2004)

[6*] Thomas, Andrew S.* W. "Control force generator", Lockheed Corporation, United States Patent 4682746, (1987)

[7] *Thomas D. Economon, William E. Milholen* II Ph.D. Thesis Stanford University, "Parametric Investigation of a 2-D Circulation Control Geometry" (2008)

[8] *Jones, G. S., Lin, J. C., Allan, B. G., Milholen, W. E., Rumsey, C. L., and Swanson, R. C.*, Overview of CFD Validation Experiments for Circulation Control at NASA," International Powered Lift Conference, London, UK, July 22-24 (2008)

[9] *Robin Schlecht, Scott Anders,* NASA Langley Research Center, "American Institute of Aeronautics and Astronautics Parametric Evaluation of Thin, Transonic Circulation-Control Airfoils", American Institute of Aeronautics and Astronautics, 2007

[10] *Alexander, M. G., Anders, S. G., Johnson, S. K., Florance, J. P., & Keller, D. F*. Trailing Edge Blowing on a Two-Dimensional Six-Percent Thick Elliptical Circulation Control Airfoil Up to Transonic Conditions. NASA/TM-2005-213545. Hampton: Langley Research Center, (2005).

[11] *Valeriu Dragan*, "A parametric study of a thick, incompressible flow over a curved surface", Volume 3 Issue 4/2011, National Aerospace Research Institute, INCAS Bulletin (2011)

[12] *Gaeta, R. J., Englar, R. J., and Avera, M*., "Development of Pneumatic Over-the-Wing Powered Lift Technology Part II: Aeroacoustics," 27th AIAA Applied Aerodynamics Conference, AIAA, San Antonio, TX, AIAA-2009-3941, (2009)

[13] *Angle, II, G., O'Hara, B., Huebsch, W., and Smith, J.*, "Experimental and Computational Investigation into the Use of the Coandã Effect on the Bell A821201 Airfoil," Applications of Circulation Control Technology, edited by R. D. Joslin and G. S. Jones, Vol. 214 of Progress in Astronautics and Aeronautics, chap. 9, American Institute of Aeronautics and Astronautics, Inc., (2006)

[14] *R. H. Nichols*, "Turbulence Models and Their Application to Complex Flows," University of Alabama at Birmingham, Revision 4.01, pp. 89

[15] *André Bakker,* Applied Computational Fluid Dynamics Lecture 10, Turbulence Models, 2005.p. 33-36

[16] Guo,B.D.;Liu,P.Q.;Qu,Q.L., Blowing Circulation Control on a Seaplane Airfoil, Recent progress in fluid dynamics research: Proceeding of the Sixth International Conference on Fluid Mechanics. AIP Conference Proceedings, Volume 1376, pp. 228-231 (2011).

[17] *M. J. Aftosmis*, "Solution Adaptive Cartesian Grid Methods for Aerodynamic Flows with Complex Geometries", von Karman Institute for Fluid Dynamics Lecture Series (1997)

[18] *Joseph Slomski and Tom Marino*, "Navy Successfully Simulates Effect that May Improve Low-Speed Maneuverability", CFD review (2003)
[19] *Florin Frunzulica, Alexandru Dumitrache, Horia Dumitrescu, Octavian Preotu*, "Flow control of separating boundary layer on the Coandã surface"4TH EUROPEAN CONFERENCE FOR AEROSPACE SCIENCES (EUCASS) (2011)
[20] K. *Duraisamyy, G. Iaccarino* Curvature correction and application of the v^2-f turbulence model to tip vortex flows, Center for Turbulence Research Annual Research Briefs (2005)